



Saturated Fat is More Metabolically Harmful for the Human Liver than Unsaturated Fat or Simple Sugars

Journal:	<i>Diabetes Care</i>
Manuscript ID	Draft
Manuscript Type:	Original Article: Pathophysiology/Complications
Date Submitted by the Author:	n/a
Complete List of Authors:	<p>Luukkonen, Panu; Helsingin Yliopisto Laaketieteellinen tiedekunta, Department of Medicine Sadevirta, Sanja; University of Helsinki, Department of Medicine Zhou, You; Cardiff University Kayser, Brandon; INSERM UMR S 1166 Ali, Ashfaq; Steno Diabetes Center AS Ahonen, Linda; Steno Diabetes Center AS Lallukka, Susanna; Helsingin Yliopisto Laaketieteellinen tiedekunta Pelloux, Véronique; INSERM UMR S 1166 Gaggini, Melania; Consiglio Nazionale delle Ricerche Area della Ricerca di Pisa Jian, Ching; Helsingin Yliopisto Laaketieteellinen tiedekunta Hakkarainen, Antti; Helsingin Yliopisto Laaketieteellinen tiedekunta Lundbom, Nina; Helsingin Yliopisto Laaketieteellinen tiedekunta Gylling, Helena; Helsingin Yliopisto Laaketieteellinen tiedekunta Salonen, Anne; Helsingin Yliopisto Laaketieteellinen tiedekunta Orešič, Matej; Steno Diabetes Center AS Hyötyläinen, Tuulia; Steno Diabetes Center AS Orho-Melander, Marju; University of Lund, Malmö General Hospital, Department of Clinical Sciences Rissanen, Aila; Helsinki University, Obesity Research Unit Gastaldelli, Amalia; CNR Institute of Clinical Physiology, Cardiometabolic Risk Laboratory; University of Texas Health Science Center at San Antonio, Division of Diabetes Clément, Karine; INSERM UMR S 1166 Hodson, Leanne; University of Oxford, OCDEM Yki-Järvinen, Hannele; University of Helsinki and Helsinki University Hospital, Department of Medicine</p>

SCHOLARONE™
Manuscripts

Saturated Fat is More Metabolically Harmful for the Human Liver than Unsaturated Fat or Simple Sugars

Short title: Diets and the liver fat

Panu K. Luukkonen^{1,2}, Sanja Sädevirta^{1,2}, You Zhou^{1,3}, Brandon Kayser⁴, Ashfaq Ali⁵, Linda Ahonen⁵, Susanna Lallukka^{1,2}, Véronique Pelloux⁴, Melania Gaggini⁶, Ching Jian⁷, Antti Hakkarainen⁸, Nina Lundbom⁸, Helena Gylling², Anne Salonen⁷, Matej Orešič^{5,9,10}, Tuulia Hyötyläinen^{5,11}, Marju Orho-Melander¹², Aila Rissanen¹³, Amalia Gastaldelli⁶, Karine Clément^{4,14}, Leanne Hodson¹⁵, Hannele Yki-Järvinen^{1,2,16}

¹Minerva Foundation Institute for Medical Research, Helsinki, Finland; ²Department of Medicine, University of Helsinki and Helsinki University Central Hospital, Helsinki, Finland; ³Systems Immunity University Research Institute and Division of Infection and Immunity, School of Medicine, Cardiff University, Cardiff, United Kingdom; ⁴Sorbonne Universités, INSERM, UMRS 1166, Nutriomics team, ICAN, F-75013, Paris, France; ⁵Steno Diabetes Center, Gentofte, Denmark; ⁶Institute of Clinical Physiology, CNR, Pisa, Italy; ⁷Immunobiology Research Program, Department of Bacteriology and Immunology, University of Helsinki; ⁸Helsinki Medical Imaging Centre, Radiology, Helsinki University Hospital and University of Helsinki; ⁹School of Medical Sciences, Örebro University, Örebro, Sweden; ¹⁰Turku Centre for Biotechnology, University of Turku and Åbo Akademi University, Turku, Finland; ¹¹Department of Chemistry, Örebro University, Örebro, Sweden; ¹²Lund University, Malmö, Sweden; ¹³Obesity Research Unit, Department of Psychiatry, Helsinki University Central Hospital; ¹⁴Assistance Publique-Hôpitaux de Paris (AP-HP), Pitié-Salpêtrière Hospital, Nutrition Department F-75013, Paris, France; ¹⁵Oxford Centre for Diabetes, Endocrinology and Metabolism, University of Oxford, Oxford, UK; ¹⁶Corresponding Author

Address correspondence to: Hannele Yki-Järvinen, MD; Biomedicum Helsinki, Haartmaninkatu
8, Room C425B, FIN - 00290 Helsinki, Finland; Phone: +358 50 427 1664; E-mail:

Hannele.Yki-Jarvinen@helsinki.fi

Word count: 4000

Number of Tables: 1

Number of Figures: 3

ABSTRACT

OBJECTIVE. Weight gain predisposes to increased intrahepatic triglycerides (IHTG) and insulin resistance (IR), but these do not occur in all obese subjects. Adipose tissue lipolysis and hepatic *de novo* lipogenesis (DNL) are the main pathways contributing to IHTG, while ceramides, which synthesis is induced by saturated fatty acids and endotoxin, are key mediators of IR. We hypothesized that dietary macronutrient composition influences the mechanisms and magnitude of weight gain-induced changes in IHTG and IR.

RESEARCH DESIGN AND METHODS. We overfed 38 overweight subjects (age 48 ± 2 , BMI 31 ± 1 kg/m², liver fat $4.7 \pm 0.9\%$) 1000 extra kilocalories/day of either saturated or unsaturated fat or simple sugars for 3 weeks. We measured IHTG (¹H-MRS), pathways contributing to IHTG (lipolysis ([²H₅]glycerol) and DNL (²H₂O) basally and during euglycemic hyperinsulinemia), IR, plasma ceramides (UPLC-MS) and endotoxemia at 0 and 3 weeks.

RESULTS. Overfeeding saturated fat increased IHTG more (+55%) than unsaturated fat (+15%) or simple sugars (+33%) despite similar increases in body weight. Simple sugars increased DNL (+98%) whilst saturated fat increased lipolysis (+11%). Saturated fat but not other diets induced IR (+23%), endotoxemia (+9%) and increased multiple plasma ceramides (+32 to +63%).

CONCLUSIONS. These data demonstrate that the macronutrient composition of the diet overconsumed matters. Saturated fat exerts greater metabolic harm on the liver than unsaturated fat or simple sugars.

Keywords: non-alcoholic fatty liver disease, diet, overfeeding, insulin resistance, adipose tissue, lipolysis, *de novo* lipogenesis, ceramides, endotoxemia

INTRODUCTION

The rapid increase in the prevalence of obesity has led to a co-epidemic of non-alcoholic fatty liver disease (NAFLD) (1). NAFLD is strongly associated with insulin resistance (IR) and predicts the development of type 2 diabetes and cardiovascular disease (CVD) (1). Whilst obesity is its primary acquired cause, some subjects who gain weight do not develop NAFLD (1,2). Whether composition of the diet contributes to susceptibility of NAFLD is unclear. Saturated but not polyunsaturated fat has been reported to increase intrahepatic triglyceride (IHTG) in young non-obese adults, despite similar weight gain (2). The epidemic of obesity has been attributed to an increased intake of simple sugars (3). However, there are no studies comparing the effects of overfeeding simple sugars, saturated or unsaturated fat diets on IHTG.

Fatty acids (FAs) in IHTG can originate from adipose tissue lipolysis, hepatic *de novo* lipogenesis (DNL) and dietary fat (4). Lipolysis provides most of the FAs used for synthesis of IHTG (4). DNL produces exclusively saturated fatty acids (SFA) from substrates such as simple sugars (4,5). Excess sugar intakes increase DNL and IHTG content in humans (5). In mice, a high-fat diet increases adipose tissue lipolysis (6). The pathway *via* which IHTG are synthesized in response to overconsuming fat has not been studied in humans.

While IHTG are commonly associated with IR, triglycerides (TGs) themselves are inert and do not confer IR (7). We have previously shown in humans that IR co-segregates with hepatic ceramides, independent of IHTG and obesity (7). Ceramides are synthesized *de novo* from SFA such as palmitate, and interfere glucose metabolism by inhibiting insulin signaling (8) and by stimulating hepatic gluconeogenesis (9). Inflammatory mediators such as endotoxins derived from gut bacteria induce IR by upregulating ceramide synthesis (10). In mice, high-fat feeding increases the proportion of endotoxin-containing bacteria in the gut, plasma concentrations of endotoxin, and induces IR (11). To our knowledge, there are no human data comparing the

effects of hypercaloric diets enriched with either saturated or unsaturated fat or simple sugars on IR, plasma ceramides, endotoxemia and gut microbiota.

In the present study, we hypothesized that the metabolic effects of a hypercaloric diet depend on the macronutrient composition. Specifically, we hypothesized that (a) overconsumption of simple sugars stimulates DNL whilst saturated fat increases lipolysis, (b) overconsumption of simple sugars and saturated fat increases availability of SFA and thereby ceramide synthesis, (c) saturated but not unsaturated fat or simple sugar diets induce endotoxemia which may further increase ceramide synthesis. Accordingly, we compared the effects of three hypercaloric (1000 extra kilocalories/day for 3 weeks) diets on (i) IHTG content, (ii) rates of DNL, (iii) rates of lipolysis, (iv) adipose tissue transcriptome, (v) plasma concentrations of ceramides, (vi) gut microbiota and a circulating marker of endotoxemia (**Figure 1A**).

RESEARCH DESIGN AND METHODS

Subjects. Subjects in this study (ClinicalTrials.gov, NCT02133144) were recruited by newspaper advertisements or by contacting subjects who previously had participated in metabolic studies. Exclusion criteria included i) type 1 or 2 diabetes, ii) pre-existing autoimmune, viral or drug-induced liver disease, iii) excessive use of alcohol (over 20g/day for women and over 30g/day for men), iv) evidence of any other acute or chronic disease, v) extreme obesity ($\text{BMI} \geq 40 \text{ kg/m}^2$), vi) use of drugs influencing glucose or lipid metabolism, vii) pregnancy or lactation. All subjects suitable for the study based on a telephone interview were invited for a screening visit. The flow chart of study subjects is shown in **Figure S1**. The nature and potential risks of the study were explained to volunteers prior to obtaining written informed consent. The ethics committee of the Helsinki University Hospital approved the study protocol.

Study design (Figure 1A). The day before the metabolic study, a blood sample was taken for measurement of background enrichment of ^2H in plasma water and VLDL-TG palmitate for measurement of DNL. Subjects then underwent measurement of IHTG by proton magnetic resonance spectroscopy (^1H -MRS). The following morning subjects arrived at the clinical research unit after an overnight fast and after consuming deuterated water ($^2\text{H}_2\text{O}$) (3g/kg body water) the evening prior to the study day, to achieve a plasma water enrichment of 0.3% for the measurement of DNL. Fecal samples were self-collected and stored immediately at -20°C and within 24 h at -80°C until analysis. Body composition (InBody 720, Biospace, Seoul, Korea), weight and height were measured and blood samples taken for measurement of DNL and for liver function tests, fasting glucose, FFA, insulin, total, HDL and LDL cholesterol and TG concentrations. Thereafter, a euglycemic hyperinsulinemic clamp combined with infusion of [$^2\text{H}_5$]glycerol for measurement of lipolysis was performed.

After the baseline visit, the subjects were randomized to one of three groups to consume a hypercaloric (1000 excess kcal/day) diet for 3 weeks with excess energy originating predominantly from either saturated fat (SAT, 76% from SFA, 21% from MUFA and 3% from PUFA), unsaturated fat (UNSAT, 57% from monounsaturated fatty acids (MUFA), 22% from polyunsaturated fatty acids (PUFA), 21% from saturated fatty acids (SFA)), or from simple sugars (CARB, 100% simple sugars). The overfeeding diets were provided to participants, and consisted in the SAT group of 30g coconut oil, 40g butter and 100g of 40% fat containing blue cheese as extra energy per day, in the UNSAT group of 36g olive oil, 26g pesto, 54g pecan nuts and 20g of butter, and in the CARB group of 2.8dL orange juice, 4.3dL of a sugar-sweetened beverage, and 200g of candy. Of the overfeeding energy, 2%, 91% and 7% came from carbohydrate, fat and protein in the UNSAT group and 1%, 86% and 13% from these sources in the SAT group, respectively and 100% from simple sugars in the CARB group. After 3 weeks of consuming the hypercaloric diets, baseline measurements were repeated.

Adherence to the diets was reinforced by weekly contacts with the study dietician, and verified by 3-day dietary records, which were performed before and after 3 weeks on the diet, and by measuring the FA composition of fasting VLDL-TG as an objective biomarker of recent dietary FA intake (12). The food records were analyzed using the AivoDiet software (version 2.0.2.3, Aivo Finland, Turku, Finland).

FA composition of VLDL-TG

VLDL was isolated by ultracentrifugation as described (5). Total lipids were extracted (13) and FA methyl esters (FAMES) prepared from TG as described (14). Separation and quantification (expressed as mol%) of FAMES was achieved on a HP6890 GC (Agilent Technologies, Stockport, UK) with flame ionisation detection.

Substrate oxidation rates

Respiratory gas exchange and rates of resting energy expenditure were recorded for 40 min before the insulin infusion and for 40 min during euglycemic hyperinsulinemia by indirect calorimetry using a computerized flow-through canopy system (Deltatrac, Datex, Helsinki, Finland) as described (15). Protein oxidation was calculated from urinary urea nitrogen excretion. Rates of carbohydrate and lipid oxidation were calculated from the gas exchange data as described (15).

IHTG and visceral and subcutaneous fat

IHTG content was determined by ^1H -MRS and visceral and subcutaneous fat by magnetic resonance imaging using 1.5T Siemens Avanto^{fit} as described (5).

DNL

Fasting DNL was assessed based on the incorporation of deuterium from $^2\text{H}_2\text{O}$ in plasma water (Finnigan GasBench-II, ThermoFisher Scientific, UK) into VLDL-TG palmitate using gas chromatography/mass spectrometry (GC/MS) with monitoring ions with mass-to-charge ratios (m/z) of 270 ($M+0$) and 271 ($M+1$) (16). Absolute DNL was calculated by multiplying %DNL and the concentration of TG in VLDL (17).

Lipolysis

Insulin action on serum FFA and glycerol rate of appearance (R_a) were determined using the euglycemic hyperinsulinemic clamp technique as previously described (5). The duration of the insulin infusion was 120 min (120-240 min) and rate of the continuous insulin infusion was 0.4 mU/kg·min.

Adipose tissue transcriptome

In the beginning of the study, after indirect calorimetry, a needle aspiration biopsy from abdominal subcutaneous adipose tissue was obtained under 1% lidocaine anesthesia and immediately frozen in liquid nitrogen and stored at -80°C until analysis. Total RNA was isolated using the RNeasy Lipid Tissue Mini Kit (Qiagen, Valencia, CA). The transcriptome was analysed using Illumina HumanHT12v4 microarray chips (Illumina, San Diego, CA). The reporter features analysis of KEGG pathway enrichment adjusted to the Benjamini-Hochberg false discovery rate (FDR) was performed using LIMMA (Bioconductor) as detailed in Supplement Material.

Plasma ceramides

Plasma lipidomic analyses were performed using a 1290 Infinity ultra-high-performance liquid chromatograph (Agilent Technologies, Santa Clara, CA) and a 6550 iFunnel quadrupole time-of-flight mass spectrometer (Agilent) as described (18).

Gut microbiota

Bacterial DNA was extracted from fecal samples and 16S rRNA was sequenced using Illumina MiSeq paired-end sequencing as detailed in Supplementary Material.

Other analytical procedures

Serum lipopolysaccharide-binding protein (LBP) and soluble cluster of differentiation 14 (sCD14) were measured by quantitative enzyme-linked immunosorbent assay (ELISA) using human LBP DuoSet® ELISA and human CD14 DuoSet® ELISA kits (both from R&D Systems, Minneapolis, MN, USA). Other analytical procedures were performed as described (18)

Statistics

Power calculation. IHTG was the primary outcome, with metabolic variables and other components of body composition considered as secondary outcomes; intestinal microbiota was an exploratory outcome. Based on a previous study (2), 14 subjects per group were needed to detect a 0.6% difference in change in liver fat between the groups with an alpha of 0.05 and beta of 0.2.

Continuous variables were tested for normality using the Kolmogorov-Smirnov method. Changes between groups were compared using one-way analysis of variance followed by a two-tailed paired Student's t-test to analyze the effect of overfeeding within each group, and a two-tailed unpaired t-test to analyze the differences between groups. Nonparametric variables were log-transformed for analysis and back-transformed for presentation, or analyzed nonparametrically with the Kruskal-Wallis test. Categorical variables were analyzed with a chi-square test. Analyses were performed with R 3.3.1 (<http://www.r-project.org/>), IBM SPSS Statistics 22.0.0.0 version (IBM, Armonk, NY) and GraphPad Prism 6.0f for Mac OS X (GraphPad Software, La Jolla, CA). Data are presented as the mean with SEMs for normally distributed variables and as medians (quartiles 1-3) for non-normally distributed variables. $P < 0.05$ were considered statistically significant.

RESULTS

Baseline characteristics

Baseline studies were performed in 39 subjects, of which 38 completed the study. The SAT, UNSAT and CARB groups were comparable with respect to age, gender, BMI, IHTG, body composition and biochemical characteristics such as glucose, insulin, lipids and liver enzymes (**Table 1**). Baseline composition of the diet (**Table S1**) and the FA composition of VLDL-TG (**Table S2**) were also comparable between the groups.

Compliance

Macronutrient composition. At the end of the overfeeding period, fat comprised 60 [54–64] and 59 [53–61] % of total energy intake in the SAT and UNSAT groups, respectively. These percentages were 2-fold higher than in the CARB group (24 [20–26] %, **Table S1**). Saturated fat intake was 2-fold higher in the SAT (33 [28–36] %) than the UNSAT (14 [14–18] % group ($p<0.001$). Monounsaturated (28 [23–30] vs. 13 [12–15] %, UNSAT vs. SAT, $p<0.001$) and polyunsaturated (11 [10–14] vs. 5 [4–5] %, respectively, $p<0.001$) fat intakes were 2-fold higher in the UNSAT than the SAT group. The % total energy intake from carbohydrate was 2.8-fold higher in the CARB (64 [58–68] %) than in the UNSAT (23 [19–29] %, $p<0.001$) or the SAT (26 [23–32] %, $p<0.001$) group.

FA composition of VLDL-TG. The FA composition of fasting plasma VLDL-TG, was used to monitor compliance (**Figure 1B**). During the SAT diet, the abundance of SFA in VLDL-TG increased significantly: 16:0 by 17% (26.2 ± 1.0 vs. 30.7 ± 1.0 mol% ($p<0.001$)), 18:0 (3.1 ± 0.3 vs. 4.1 ± 0.3 mol% ($p<0.01$)) and 14:0 (1.8 ± 0.2 vs. 4.8 ± 0.5 mol% ($p<0.001$)). The abundance of 18:2 decreased significantly during the SAT diet. During the UNSAT diet, 18:2 increased significantly ($p<0.01$). During the CARB diet, the abundance of 16:0, 14:0 and 16:1 increased and 18:2 decreased significantly ($p<0.05$) (**Figure 1B**).

Body weight and composition

In all subjects, body weight increased by 1.4 ± 0.2 % from 92.1 ± 2.8 to 93.3 ± 2.8 kg ($p < 0.001$). Changes in body weight averaged 1.4 ± 0.3 kg in the SAT, 0.9 ± 0.3 kg in the UNSAT and 1.4 ± 0.5 kg in the CARB groups ($p = \text{NS}$). In all subjects, intra-abdominal and subcutaneous fat did not change significantly during overfeeding (data not shown).

Energy expenditure and substrate oxidation rates

All subjects. As expected, overfeeding increased resting energy expenditure significantly from 7.49 ± 0.22 to 7.62 ± 0.24 MJ/day ($p < 0.05$) in all subjects. Rates of energy expenditure and substrate oxidation rates expressed per kg body weight or fat free mass remained unchanged in all subjects, within and between groups (data not shown). Non-protein respiratory quotient (NPRQ) did not change with overfeeding (data not shown).

Intrahepatic triglyceride

IHTG increased by 55% (4.9 ± 1.8 vs. $7.6 \pm 2.4\%$ ($p < 0.001$)) in the SAT group, by 15% (4.8 ± 1.4 vs. $5.5 \pm 1.4\%$ ($p < 0.02$)) in the UNSAT group, and by 33% (4.3 ± 1.3 vs. $5.7 \pm 1.6\%$ ($p < 0.02$)) in the CARB group (**Figure 1C**). The increase was significantly greater in the SAT than the UNSAT ($p < 0.01$) or the CARB groups ($p < 0.05$) (**Figure 1D**).

***De novo* lipogenesis**

Hepatic DNL, as determined by the amount of newly synthesized palmitate in VLDL-TG, increased significantly during the CARB diet (96 [47 – 116] vs. 190 [61 – 303] $\mu\text{mol/L}$, $p < 0.05$) but not other diets (**Figure 2A**).

Lipolysis

Basal state. Fasting serum insulin increased significantly with overfeeding in the SAT group (10.7 ± 2.8 vs. 12.9 ± 2.9 mU/L, $p < 0.02$) but remained unchanged in the UNSAT (10.4 ± 1.4 vs. 10.6 ± 1.5 mU/L, NS) and CARB (14.5 ± 3.5 vs. 15.3 ± 3.6 mU/L, NS) groups. Basal whole-body glycerol R_a remained unchanged in all groups (**Figure 2B**).

Euglycemic hyperinsulinemia. During hyperinsulinemia, increases in serum insulin concentrations were similar before and after the diets (22 ± 1 vs. 22 ± 1 mU/L, $p = \text{NS}$) with no differences between the SAT, UNSAT and CARB groups (data not shown). Whole-body glycerol R_a during euglycemic hyperinsulinemia compared to baseline increased in SAT (2.08 ± 0.12 vs. 2.31 ± 0.16 $\mu\text{mol/kg} \cdot \text{min}$, $p < 0.05$), decreased in the UNSAT (2.59 ± 0.25 vs. 2.14 ± 0.22 $\mu\text{mol/kg} \cdot \text{min}$, $p < 0.05$), and remained unchanged in the CARB (2.15 ± 0.21 vs. 2.27 ± 0.19 $\mu\text{mol/kg} \cdot \text{min}$, NS) group after overfeeding (**Figure 2C**). Insulin-induced suppression of whole-body glycerol R_a increased significantly more in the SAT compared to the UNSAT ($p < 0.001$) and the CARB compared to the UNSAT ($p < 0.01$) group (**Figure 2C**).

Serum FFA. Serum FFA concentrations, which reflect the net effects of lipolysis and lipogenesis, remained unchanged in the SAT group but decreased significantly during hyperinsulinemia by overfeeding in the UNSAT and CARB groups (**Figure S2**).

Adipose tissue transcriptome

Gene set analysis identified 28 reporter pathways out of 134 curated KEGG pathways at a 5% FDR. The SAT and CARB diets changed 18, while the UNSAT diet changed 5 pathways, which were highly distinctive between the diets. Only 3 pathways overlapped between all diets (**Figure 2D**). The pathways upregulated by the SAT diet included those related to inflammation, such as genes related to *E. coli* infection, natural killer cell-mediated cytotoxicity, NOD-like receptor

signaling and leukocyte transendothelial migration, and to glycerolipid metabolism. The SAT and CARB diets shared some pathways related to inflammation, such as genes related to antigen processing, chemokine signaling, and hematopoietic cell lineage. In addition, CARB induced pathways related to carbohydrate metabolism such as fructose and mannose metabolism, pentose phosphate pathway and glycolysis/gluconeogenesis. The UNSAT diet upregulated pathways related to oxidative phosphorylation and extracellular matrix.

Insulin resistance and plasma ceramides

In the SAT group, HOMA-IR increased significantly by 23% (1.9 [1.3–3.2] vs. 2.2 [1.4–3.3], $p<0.05$), and remained unchanged in the UNSAT and CARB groups (**Figure 3A**).

In the SAT group, total plasma ceramide concentration increased significantly by 49% ($p<0.001$, **Figure 3B**). In contrast, there were no changes in plasma ceramides in the UNSAT or CARB groups. The increase in total plasma ceramide concentration in the SAT group was due to increases in several long-chain ceramides (**Figure 3D, Table S3**). Plasma concentrations of dihydroceramides (i.e. the precursors of ceramides in the *de novo* ceramide synthetic pathway, the species with 18:0 sphingoid base) were also increased in the SAT but not the other groups (**Figure 3D, Table S3**).

Gut microbiota and LBP/sCD14

Serum LBP/sCD14, a marker of endotoxemia (19), increased significantly (4.3 ± 0.3 vs. 4.7 ± 0.3 ($p<0.01$)) in the SAT group and remained unchanged in the UNSAT and CARB groups (**Figure 3C**). Serum LBP tended to increase (from 4.5 [4.2–5.8] to 5.2 [4.6–6.0] ng/mL, $p=0.11$) in the SAT but not the other groups.

Regarding gut microbiota, most (79%) of between-sample microbiota variation was explained by the subject ($p<0.001$, **Figure S3**), highlighting overall resilience of the individual-specific microbiota during overfeeding. We next analyzed individual taxa that were affected by overfeeding (**Figure S4**). The abundance of gram-negative Proteobacteria increased 3.6-fold during the SAT ($p=0.038$) but not the other diets (**Figure S5**). Other bacterial families remained unchanged.

Plasma lipids

Baseline lipid concentrations are shown in **Table 1**. Plasma HDL cholesterol increased significantly by 17% in the SAT ($+0.3\pm0.1$ mmol/l, $p<0.01$ for after vs. before) but not in the UNSAT ($+0.1\pm0.1$ mmol/l) or CARB (-0.1 ± 0.1 mmol/l) groups. The increase in HDL cholesterol was significantly greater in the SAT than the CARB group ($p<0.001$). Plasma LDL cholesterol increased by 10% in the SAT group ($+0.3\pm0.1$ mmol/l, $p<0.01$) but remained unchanged in the CARB and UNSAT groups. There were no significant changes in plasma triglycerides within or between the groups.

DISCUSSION

NAFLD has become ‘another disease of affluence’ but does not develop in all overweight subjects (1,2). In the present study, we examined whether the macronutrient composition of the diet influences the metabolic response to overfeeding. Consumption of a hypercaloric diet for 3 weeks increased IHTG content significantly; the diet enriched with saturated fat (SAT) induced a greater increase in IHTG than those enriched with either unsaturated fat (UNSAT) or simple sugars (CARB). The composition of the diet altered the sources of IHTG, as adipose tissue lipolysis increased only by the SAT diet, while only the CARB diet stimulated hepatic DNL. The SAT diet was the only diet to induce insulin resistance, endotoxemia and an increase in plasma ceramides.

Compliance. The sources of FA and their composition in liver TG are similar to those in VLDL secreted from the liver after an overnight fast (4). We analyzed changes in FA composition of VLDL-TG as biomarkers of compliance and of hepatic FA composition. The SAT diet increased SFA and decreased polyunsaturated FA while the UNSAT diet increased polyunsaturated FA (**Figure 1B**). The CARB diet also increased SFA, which are exclusive products of DNL (5), and decreased polyunsaturated FAs in VLDL-TG. These data demonstrate that subjects were compliant, and are novel in showing that different diets have distinct effects on hepatic FA composition as determined from that in VLDL-TG.

IHTG. Overfeeding has been reported to increase IHTG content (2,5,20). We extend previous findings by showing that the magnitude, pathways and possible mediators *via* which overfeeding influences IHTG depends on composition of the diet. The SAT diet increased IHTG significantly more than the other two diets even though excess energy intake and changes in body weight were similar in all groups. The greater increase in IHTG in the SAT group as compared to the UNSAT group is consistent with a previous study showing a significantly

greater increase in IHTG after overfeeding saturated as compared to polyunsaturated fat (2). In a study comparing isocaloric diets, saturated fat-enriched diet increased IHTG compared to that enriched in polyunsaturated fat (21). We (22), and others (23) have shown that high saturated fat intakes characterize subjects with NAFLD. Together these studies imply that diet composition influences the extent of ectopic fat deposition in the liver and that saturated fat induces greater accumulation of IHTG than unsaturated fat.

Pathways of IHTG. Regarding the causes underlying increased deposition of FAs into IHTG during overconsumption of SFA, pathways leading to IHTG need to be considered. Direct quantification of sources of FAs in IHTG using stable isotopes and liver biopsies in subjects with elevated IHTG have shown that the majority of IHTG are derived from adipose tissue lipolysis (59%) and DNL (26%) (4). We demonstrate here that adipose tissue lipolysis increases in response to SAT but not UNSAT or CARB diets. Lipolysis was traced using deuterated glycerol. Glycerol was chosen, as it is not re-esterified in adipose tissue due to a lack of glycerol kinase. This is in contrast to FFA whose circulating concentration reflects net effects of lipolysis and lipogenesis. Serum FFA decreased in response to overfeeding, as in a previous study (20). We are not aware of overfeeding studies measuring lipolysis in humans, but in mice high-fat feeding stimulates lipolysis (6). The increase in lipolysis could be a consequence of SFA-induced inflammation in adipose tissue (24), which is supported by the adipose tissue transcriptome data showing upregulation of multiple inflammation-related pathways during the SAT diet. The ability of the SAT but not UNSAT or CARB diet to stimulate lipolysis, the major contributor to IHTG, could explain why SAT increased IHTG to a greater extent than the two other diets.

Overfeeding simple sugars stimulates DNL, which produces exclusively SFA in humans and occurs mainly in the liver (5). Consistent with these data, the CARB diet increased hepatic DNL

and SFAs in VLDL-TG (**Figures 1B and 2A**). Stimulation of DNL was, however, not able to increase IHTG as much as the SAT diet which increased lipolysis. This is consistent with a greater increase in IHTG by isocaloric high-fat, low-carbohydrate as compared to low-fat, high-carbohydrate diets lasting for two (25), three (26) and four (27) weeks in humans.

IR and its mediators. Only the SAT diet induced IR. Cross-sectionally, intakes of SFA have been shown to associate with IR (23). In addition, several studies have shown that isocaloric substitution of saturated for monounsaturated fat (28-29), carbohydrates (29), or polyunsaturated fat (30) ameliorates IR. Recently, a large prospective study reported intake of foods rich in SFA such as butter and cheese to increase the risk of type 2 diabetes (31). Even a single meal enriched with SFA is sufficient to induce IR in mice and humans (32).

TGs themselves are inert and do not confer IR (7). In mice, ceramides are key mediators of saturated fat-induced IR (8-10,33-36). We have previously reported that ceramides are the most upregulated lipid species in inflamed adipose tissue of subjects with NAFLD compared to age-, gender- and body weight-matched subjects (37), and that SFAs, dihydroceramides (markers of *de novo* ceramide synthesis) and ceramides co-segregate with IR in the human liver (7).

De novo ceramide synthesis is upregulated by substrate availability, i.e. palmitoyl-CoA (8, 33), and by ligands of the Toll-like receptor 4, such as endotoxin, a component of gram-negative bacteria (8,10). Infusion of endotoxin induces adipose tissue inflammation (11) and ceramide-dependent IR (10). Endotoxemia occurs in humans in response to a single high-saturated fat meal (38). In the present study, the SAT diet was the only diet that enriched fecal gram-negative Proteobacteria, increased circulating markers of endotoxemia, upregulated genes related to gram-negative bacterial infection in the adipose tissue, stimulated lipolysis, increased plasma concentrations of dihydroceramides and ceramides, and induced IR. These data suggest that *de*

novo synthesis of ceramides induced by SFA and endotoxin could contribute to saturated fat-induced IR. Lack of endotoxemia in the CARB group may explain why ceramides failed to increase in this group.

The present data showing that SAT stimulates adipose tissue lipolysis and induces IR also supports the "single gateway hypothesis" which proposes that hepatic glucose production is indirectly regulated by FFA originating from adipose tissue (6,39).

In conclusion, overfeeding either saturated or unsaturated fat or simple sugars for 3 weeks increases IHTG content but the magnitude of this response and the associated metabolic changes depend on the quality of the diet. Consistent with current dietary recommendations, saturated fat seems most harmful not just in terms of the risk of diabetes and CVD but also in terms of NAFLD. Saturated but not unsaturated fat or simple sugars increased adipose tissue lipolysis, circulating ceramides and induced endotoxemia and insulin resistance. These data do not negate a role of carbohydrates in causing NAFLD. The obesity and NAFLD epidemics are undoubtedly consequences of overconsumption of potato chips, sugar-sweetened beverages and other sugars rather than saturated fat (3). However, the present study shows that when compared in the face of similar energy excess, saturated fats are the most harmful constituents in the diet regarding liver health and echo the recommendation of consuming unsaturated rather than saturated fats.

ACKNOWLEDGEMENTS

Author Contributions. P.L.: clinical research conduction, acquisition, analysis and interpretation of data, drafting and critical revision of the manuscript; S.S.: study diet design, clinical research conduction, critical revision of the manuscript; Y.Z., B.K.: analysis and interpretation of the data, critical revision of the manuscript; A.A., L.A., S.L., V.P., M.G., C.J., A.H., N.L., H.G., M.O., T.H., A.G., M.O-M., K.C.: acquisition of data, critical revision of the

manuscript; A.S., A.R., L.H.: acquisition, analysis and interpretation of data, critical revision of the manuscript; H.Y-J.: study concept and design, analysis and interpretation of the data, drafting and critical revision of the manuscript; study supervision. H.Y-J. is the guarantor of this work and, as such, had full access to all the data in the study and takes responsibility for the integrity of the data and the accuracy of the data analysis.

The authors gratefully acknowledge Anne Salo, Aila Karioja-Kallio, Pentti Pölönen, Leena Kaipiainen and Raisa Harjula (Helsinki University Hospital) as well as Catriona Charlton (University of Oxford) for skillful technical assistance, A. Margot Umpleby (University of Surrey) for advice on stable isotope methodology, and Siiri Luukkonen for graphical assistance.

Duality of Interest. The authors have declared that no conflict of interest exists.

Funding. This study was supported by grants from the University of Helsinki (PL, AS), the EU/EFPIA Innovative Medicines Initiative Joint Undertaking (EMIF grant no. 115372, HY), the EPoS (Elucidating Pathways of Steatohepatitis) consortium funded by the Horizon 2020 Framework Program of the European Union under Grant Agreement 634413 (HY, AG, TH, MO, KC, BK), MIUR and CNR (AG), the British Heart Foundation Intermediate Fellowship in Basic Science (FS/11/18/28633) (LH), PIA- F-Crin Force program (KC, VP), Academy of Finland (HY), the Sigrid Juselius (HY), EVO (HY), the Finnish Medical (PL), the Yrjö Jahnsson (PL) and Novo Nordisk (HY) Foundations.

Prior presentation. Parts of this study were presented in abstract form at the 52nd Annual Meeting of the European Association for the Study of Diabetes, Munich, Germany, 12-16 September 2016 and 77th Scientific Sessions of the American Diabetes Association, San Diego, CA, 9-13 June 2017.

Figure Legends

Figure 1. (A) Design of the study, (B) overfeeding-induced changes in fatty acid (FA) composition of VLDL-TG in the groups, (C) intrahepatic triglyceride (IHTG) before and after overfeeding, and (D) changes in IHTG between the groups. The subjects were randomized into overfeeding either saturated fat (SAT), unsaturated fat (UNSAT), or simple sugars (CARB). All subjects underwent metabolic studies at baseline and after 3 weeks of overfeeding. At these visits, intrahepatic triglyceride content was determined by proton magnetic resonance spectroscopy (^1H -MRS), hepatic *de novo* lipogenesis from $^2\text{H}_2\text{O}$ enrichment in VLDL-TG palmitate, adipose tissue lipolysis by $^2\text{H}_5$ -glycerol in the basal state and during euglycemic hyperinsulinemia, plasma ceramides by UHPLC-MS, and endotoxemia by 16S rRNA and serum LBP/sCD14 ELISA. In addition, adipose tissue transcriptome was determined by microarray. Black bars denote the SAT group, white bars the UNSAT, and hatched bars the CARB group. In (B), the x-axis shows the change in % FA in VLDL-TG after versus before overfeeding and the y-axis the specific fatty acids in VLDL-TG. Data are shown as mean \pm SEM. * $p < 0.05$, ** $p < 0.01$, *** $p < 0.001$. B = before, A = after.

Figure 2. Overfeeding-induced changes in (A) hepatic *de novo* lipogenesis, (B) basal glycerol rate of appearance (R_a), (C) glycerol R_a during euglycemic hyperinsulinemia, and (D) adipose tissue transcriptome. Black bars denote the saturated fat (SAT), white bars the unsaturated fat (UNSAT), and hatched bars the simple sugar (CARB) group. The y-axes indicate fold-change of mean values after versus before overfeeding within groups. Data are reported as mean \pm SEM. * $p < 0.05$, ** $p < 0.01$, *** $p < 0.001$. X = $p < 0.05$ between groups. The bubble grid shows the reporter test statistics (proportional to size and color intensity) comparing post- relative to pre-overfeeding gene expression. Only pathways significant in at least one diet are shown ($< 5\%$ false discovery rate).

Figure 3. Overfeeding-induced changes in (A) HOMA-IR, (B) total plasma ceramides, (C) LBP/sCD14, and (D) individual plasma ceramides in the groups. Black bars denote the saturated fat (SAT), white bars the unsaturated fat (UNSAT), and hatched bars the simple sugar (CARB) group. The y-axes indicate fold-change of mean values after versus before overfeeding within groups. HOMA-IR = homeostasis model of assessment of insulin resistance, LBP/sCD14 = ratio of lipopolysaccharide-binding protein to soluble cluster of differentiation 14. Data are reported as mean \pm SEM. In the heatmaps, each square indicates the \log_2 of the ratio between mean concentrations after versus before for an individual ceramide. The color key denotes the relationship between the color of the heatmap and \log_2 of the ratio between the means with 0 indicating no change. The y-axis denotes the fatty acyl chain structure (number of carbon atoms:number of double bonds) and the x-axis the sphingoid base species. * $p < 0.05$, ** $p < 0.01$, *** $p < 0.001$.

REFERENCES

1. Yki-Järvinen H. Non-alcoholic fatty liver disease as a cause and a consequence of metabolic syndrome. *Lancet Diabetes Endocrinol*. 2014;2(11):901-10.
2. Rosqvist F, Iggman D, Kullberg J, Cedernaes J, Johansson HE, Larsson A, Johansson L, Ahlström H, Arner P, Dahlman I, Risérus U. Overfeeding polyunsaturated and saturated fat causes distinct effects on liver and visceral fat accumulation in humans. *Diabetes*. 2014;63(7):2356-68.
3. Mozaffarian D, Hao T, Rimm EB, Willett WC, Hu FB. Changes in diet and lifestyle and long-term weight gain in women and men. *N Engl J Med*. 2011;364(25):2392-404.
4. Donnelly KL, Smith CI, Schwarzenberg SJ, Jessurun J, Boldt MD, Parks EJ. Sources of fatty acids stored in liver and secreted via lipoproteins in patients with nonalcoholic fatty liver disease. *J Clin Invest*. 2005;115(5):1343-51.
5. Sevastianova K, Santos A, Kotronen A, Hakkarainen A, Makkonen J, Silander K, Peltonen M, Romeo S, Lundbom J, Lundbom N, Olkkonen VM, Gylling H, Fielding BA, Rissanen A, Yki-Järvinen H. Effect of short-term carbohydrate overfeeding and long-term weight loss on liver fat in overweight humans. *Am J Clin Nutr*. 2012;96(4):727-34.
6. Perry RJ, Camporez JP, Kursawe R, Titchenell PM, Zhang D, Perry CJ, Jurczak MJ, Abudukadier A, Han MS, Zhang XM, Ruan HB, Yang X, Caprio S, Kaech SM, Sul HS, Birnbaum MJ, Davis RJ, Cline GW, Petersen KF, Shulman GI. Hepatic acetyl CoA links adipose tissue inflammation to hepatic insulin resistance and type 2 diabetes. *Cell*. 2015;160(4):745-58.
7. Luukkonen PK, Zhou Y, Sädevirta S, Leivonen M, Arola J, Orešič M, Hyötyläinen T, Yki-Järvinen H. Hepatic ceramides dissociate steatosis and insulin resistance in patients with non-alcoholic fatty liver disease. *J Hepatol*. 2016;64(5):1167-1175.
8. Chavez JA, Summers SA. A ceramide-centric view of insulin resistance. *Cell Metab*. 2012;15(5):585-94.
9. Xie C, Jiang C, Shi J, Gao X, Sun D, Sun L, Wang T, Takahashi S, Anitha M, Krausz KW, Patterson AD, Gonzalez FJ. An Intestinal Farnesoid X Receptor-Ceramide Signaling Axis Modulates Hepatic Gluconeogenesis in Mice. *Diabetes*. 2017;66(3):613-626.
10. Holland WL, Bikman BT, Wang LP, Yuguang G, Sargent KM, Bulchand S, Knotts TA, Shui G, Clegg DJ, Wenk MR, Pagliassotti MJ, Scherer PE, Summers SA. Lipid-induced insulin resistance mediated by the proinflammatory receptor TLR4 requires saturated fatty acid-induced ceramide biosynthesis in mice. *J Clin Invest*. 2011;121(5):1858-70.
11. Cani PD, Amar J, Iglesias MA, Poggi M, Knauf C, Bastelica D, Neyrinck AM, Fava F, Tuohy KM, Chabo C, Waget A, Delmée E, Cousin B, Sulpice T, Chamontin B, Ferrières J, Tanti JF, Gibson GR, Casteilla L, Delzenne NM, Alessi MC, Burcelin R. Metabolic endotoxemia initiates obesity and insulin resistance. *Diabetes*. 2007;56(7):1761-72.
12. Hodson L, Skeaff CM, Fielding BA. Fatty acid composition of adipose tissue and blood in humans and its use as a biomarker of dietary intake. *Prog Lipid Res*. 2008;47(5):348-80.
13. Folch J, Lees M, Sloane Stanley GH. (1957). A simple method for the isolation and purification of total lipides from animal tissues. *J Biol Chem*. 226(1): 497-509.
14. Heath RB, Karpe F, Milne RW, et al. (2003). Selective partitioning of dietary fatty acids into the VLDL TG pool in the early postprandial period. *J Lipid Res*. 44(11):2065-72.
15. Yki-Järvinen H, Puhakainen I, Saloranta C, Groop L, Taskinen MR. Demonstration of a novel feedback mechanism between FFA oxidation from intracellular and intravascular sources. *Am J Physiol*. 1991;260(5 Pt 1):E680-9.
16. Semple RK, Sleight A, Murgatroyd PR, et al. (2009). Postreceptor insulin resistance contributes to human dyslipidemia and hepatic steatosis. *J Clin Invest*. 119(2):315-22.
17. Santoro N, Caprio S, Pierpont B, et al. (2015). Hepatic De Novo Lipogenesis in Obese Youth Is Modulated by a Common Variant in the GCKR Gene. *J Clin Endocrinol Metab*. 100(8):E1125-32.

18. Luukkonen PK, Zhou Y, Nidhina Haridas PA, Dwivedi OP, Hyötyläinen T, Ali A, Juuti A, Leivonen M, Tukiainen T, Ahonen L, Scott E, Palmer JM, Arola J, Orho-Melander M, Vikman P, Anstee QM, Olkkonen VM, Orešić M, Groop L, Yki-Järvinen H. Impaired hepatic lipid synthesis from polyunsaturated fatty acids in TM6SF2 E167K variant carriers with NAFLD. *J Hepatol*. 2017;67(1):128-136.
19. Laugerette F, Alligier M, Bastard JP, Draï J, Chanséaume E, Lambert-Porcheron S, Laville M, Morio B, Vidal H, Michalski MC. Overfeeding increases postprandial endotoxemia in men: Inflammatory outcome may depend on LPS transporters LBP and sCD14. *Mol Nutr Food Res*. 2014;58(7):1513-8.
20. Sobrecases H, Lê KA, Bortolotti M, Schneiter P, Ith M, Kreis R, Boesch C, Tappy L. Effects of short-term overfeeding with fructose, fat and fructose plus fat on plasma and hepatic lipids in healthy men. *Diabetes Metab*. 2010;36(3):244-6.
21. Bjermo H, Iggman D, Kullberg J, Dahlman I, Johansson L, Persson L, Berglund J, Pulkki K, Basu S, Uusitupa M, Rudling M, Arner P, Cederholm T, Ahlström H, Risérus U. Effects of n-6 PUFAs compared with SFAs on liver fat, lipoproteins, and inflammation in abdominal obesity: a randomized controlled trial. *Am J Clin Nutr*. 2012;95(5):1003-12.
22. Tiikkainen M, Bergholm R, Vehkavaara S, Rissanen A, Häkkinen AM, Tamminen M, Teramo K, Yki-Järvinen H. Effects of identical weight loss on body composition and features of insulin resistance in obese women with high and low liver fat content. *Diabetes*. 2003;52(3):701-7.
23. Musso G, Gambino R, De Michieli F, Cassader M, Rizzetto M, Durazzo M, Fagà E, Silli B, Pagano G. Dietary habits and their relations to insulin resistance and postprandial lipemia in nonalcoholic steatohepatitis. *Hepatology*. 2003;37(4):909-16.
24. van Dijk SJ, Feskens EJ, Bos MB, Hoelen DW, Heijligenberg R, Bromhaar MG, de Groot LC, de Vries JH, Müller M, Afman LA. A saturated fatty acid-rich diet induces an obesity-linked proinflammatory gene expression profile in adipose tissue of subjects at risk of metabolic syndrome. *Am J Clin Nutr*. 2009;90(6):1656-64.
25. Westerbacka J, Lammi K, Häkkinen AM, Rissanen A, Salminen I, Aro A, Yki-Järvinen H. Dietary fat content modifies liver fat in overweight nondiabetic subjects. *J Clin Endocrinol Metab*. 2005;90(5):2804-9.
26. van Herpen NA, Schrauwen-Hinderling VB, Schaart G, Mensink RP, Schrauwen P. Three weeks on a high-fat diet increases intrahepatic lipid accumulation and decreases metabolic flexibility in healthy overweight men. *J Clin Endocrinol Metab*. 2011;96(4):E691-5.
27. Utzschneider KM, Bayer-Carter JL, Arbuckle MD, Tidwell JM, Richards TL, Craft S. Beneficial effect of a weight-stable, low-fat/low-saturated fat/low-glycaemic index diet to reduce liver fat in older subjects. *Br J Nutr*. 2013;28;109(6):1096-104.
28. Vessby B, Uusitupa M, Hermansen K, Riccardi G, Rivellese AA, Tapsell LC, Näslén C, Berglund L, Louheranta A, Rasmussen BM, Calvert GD, Maffetone A, Pedersen E, Gustafsson IB, Storlien LH; KANWU Study. Substituting dietary saturated for monounsaturated fat impairs insulin sensitivity in healthy men and women: The KANWU Study. *Diabetologia*. 2001;44(3):312-9.
29. Pérez-Jiménez F, López-Miranda J, Pinillos MD, Gómez P, Paz-Rojas E, Montilla P, Marín C, Velasco MJ, Blanco-Molina A, Jiménez Perepérez JA, Ordovás JM. A Mediterranean and a high-carbohydrate diet improve glucose metabolism in healthy young persons. *Diabetologia*. 2001;44(11):2038-43.
30. Summers LK, Fielding BA, Bradshaw HA, Ilic V, Beysen C, Clark ML, Moore NR, Frayn KN. Substituting dietary saturated fat with polyunsaturated fat changes abdominal fat distribution and improves insulin sensitivity. *Diabetologia*. 2002;45(3):369-77.
31. Guasch-Ferré M, Becerra-Tomás N, Ruiz-Canela M, Corella D, Schröder H, Estruch R, Ros E, Arós F, Gómez-Gracia E, Fiol M, Serra-Majem L, Lapetra J, Basora J, Martín-Calvo N, Portoles O, Fitó M, Hu FB, Forga L, Salas-Salvadó J. Total and subtypes of dietary fat intake and

risk of type 2 diabetes mellitus in the Prevención con Dieta Mediterránea (PREDIMED) study. *Am J Clin Nutr.* 2017;105(3):723-735.

32. Hernández EÁ, Kahl S, Seelig A, Begovatz P, Irmeler M, Kupriyanova Y, Nowotny B, Nowotny P, Herder C, Barosa C, Carvalho F, Rozman J, Neschen S, Jones JG, Beckers J, de Angelis MH, Roden M. Acute dietary fat intake initiates alterations in energy metabolism and insulin resistance. *J Clin Invest.* 2017;127(2):695-708.

33. Holland WL, Brozinick JT, Wang LP, Hawkins ED, Sargent KM, Liu Y, Narra K, Hoehn KL, Knotts TA, Siesky A, Nelson DH, Karathanasis SK, Fontenot GK, Birnbaum MJ, Summers SA. Inhibition of ceramide synthesis ameliorates glucocorticoid-, saturated-fat-, and obesity-induced insulin resistance. *Cell Metab.* 2007;5(3):167-79.

34. Raichur S, Wang ST, Chan PW, Li Y, Ching J, Chaurasia B, Dogra S, Öhman MK, Takeda K, Sugii S, Pewzner-Jung Y, Futerman AH, Summers SA. CerS2 haploinsufficiency inhibits β -oxidation and confers susceptibility to diet-induced steatohepatitis and insulin resistance. *Cell Metab.* 2014;20(4):687-95.

35. Turpin SM, Nicholls HT, Willmes DM, Mourier A, Brodesser S, Wunderlich CM, Mauer J, Xu E, Hammerschmidt P, Brönneke HS, Trifunovic A, LoSasso G, Wunderlich FT, Kornfeld JW, Blüher M, Krönke M, Brüning JC. Obesity-induced CerS6-dependent C16:0 ceramide production promotes weight gain and glucose intolerance. *Cell Metab.* 2014;20(4):678-86.

36. Xia JY, Holland WL, Kusminski CM, Sun K, Sharma AX, Pearson MJ, Sifuentes AJ, McDonald JG, Gordillo R, Scherer PE. Targeted Induction of Ceramide Degradation Leads to Improved Systemic Metabolism and Reduced Hepatic Steatosis. *Cell Metab.* 2015;22(2):266-278.

37. Kolak M, Westerbacka J, Velagapudi VR, Wågsäter D, Yetukuri L, Makkonen J, Rissanen A, Häkkinen AM, Lindell M, Bergholm R, Hamsten A, Eriksson P, Fisher RM, Oresic M, Yki-Järvinen H. Adipose tissue inflammation and increased ceramide content characterize subjects with high liver fat content independent of obesity. *Diabetes.* 2007;56(8):1960-8.

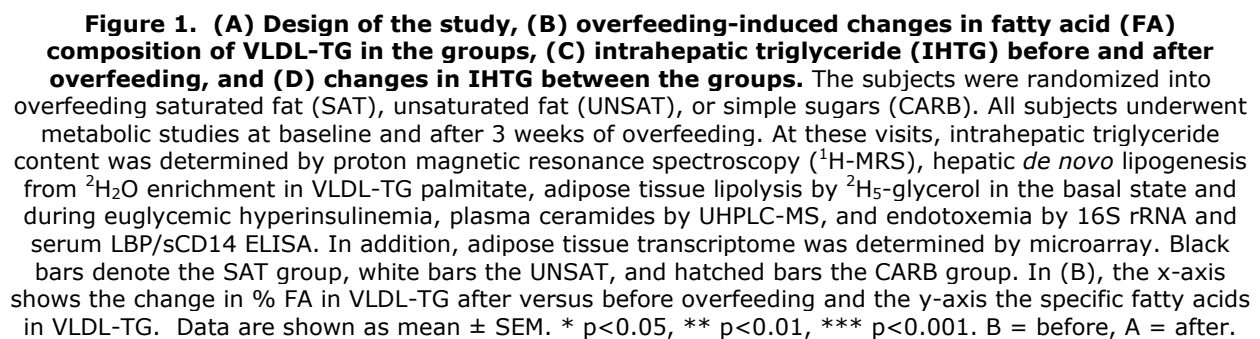
38. Deopurkar R, Ghanim H, Friedman J, Abuaysheh S, Sia CL, Mohanty P, Viswanathan P, Chaudhuri A, Dandona P. Differential effects of cream, glucose, and orange juice on inflammation, endotoxin, and the expression of Toll-like receptor-4 and suppressor of cytokine signaling-3. *Diabetes Care.* 2010;33(5):991-7.

39. Bergman RN, Iyer MS. Indirect Regulation of Endogenous Glucose Production by Insulin: The Single Gateway Hypothesis Revisited. *Diabetes.* 2017;66(7):1742-1747.

Table 1. Baseline clinical characteristics of the study subjects according to diet group.

Total	SAT (n=14)	UNSAT (n=12)	CARB (n=12)
Age (years)	48 ± 2	52 ± 3	45 ± 3
Gender (n, women/men)	8/6	7/5	6/6
BMI (kg/m ²)	30 ± 2	31 ± 2	33 ± 2
Fat free mass (kg)	58.6 ± 2.6	60.2 ± 3.8	61.9 ± 3.6
Liver fat (¹ H-MRS, %)	4.9 ± 1.8	4.8 ± 1.4	4.3 ± 1.3
Visceral adipose tissue (MRI, cm ²)	1940 ± 429	2019 ± 383	2014 ± 351
Subcutaneous adipose tissue (MRI, cm ²)	4770 ± 575	4732 ± 708	5133 ± 622
Waist circumference (cm)	97 ± 5	98 ± 4	102 ± 3
Waist to hip ratio	0.90 ± 0.03	0.90 ± 0.02	0.92 ± 0.02
LBP/CD14	4.3 ± 0.3	4.6 ± 0.3	4.9 ± 0.5
fP-Glucose (mmol/l)	5.6 ± 0.2	5.7 ± 0.2	5.9 ± 0.2
fS-Insulin (mU/l)	8.1 (5.8 – 11.9)	9.1 (6.5 – 14.6)	10.3 (6.2 – 19.2)
HOMA-IR	1.9 (1.3 – 3.2)	2.3 (1.6 – 4.0)	2.8 (1.7 – 5.0)
Systolic BP (mmHg)	133 ± 4	134 ± 5	139 ± 6
Diastolic BP (mmHg)	80 ± 3	83 ± 2	85 ± 4
fP-Triglycerides (mmol/l)	1.1 ± 0.3	1.1 ± 0.1	1.4 ± 0.2
fP-HDL cholesterol (mmol/l)	1.62 ± 0.10	1.61 ± 0.14	1.53 ± 0.11
fP-LDL cholesterol (mmol/l)	3.2 ± 0.3	3.4 ± 0.2	3.5 ± 0.2
fS-FFA (μmol/l)	556 ± 58	610 ± 52	639 ± 65
fP-ALT (IU/l)	28 ± 4	26 ± 3	24 ± 3
fP-AST (IU/l)	26 ± 1	27 ± 2	26 ± 2
PNPLA3 (CC/CG/GG) (n)	9/5/0	7/4/1	5/4/2

Data are in n (%), means ± SEM or median (25th-75th percentile), as appropriate. There were no significant differences in any variable between the groups using ANOVA, Kruskal-Wallis and Chi-squared test, as appropriate.



CONFIDENTIAL-For Peer Review Only

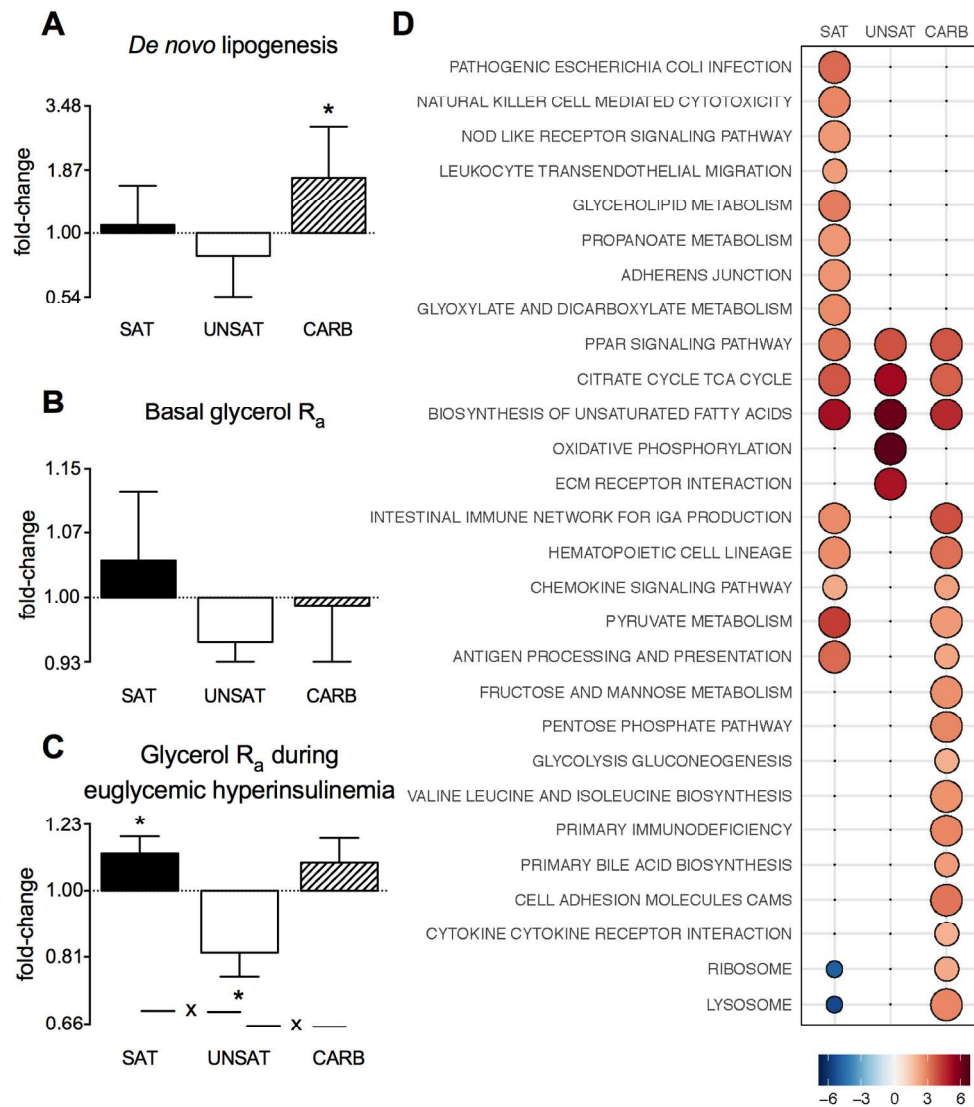


Figure 2. Overfeeding-induced changes in (A) hepatic *de novo* lipogenesis, (B) basal glycerol rate of appearance (R_a), (C) glycerol R_a during euglycemic hyperinsulinemia, and (D) adipose tissue transcriptome. Black bars denote the saturated fat (SAT), white bars the unsaturated fat (UNSAT), and hatched bars the simple sugar (CARB) group. The y-axes indicate fold-change of mean values after versus before overfeeding within groups. Data are reported as mean \pm SEM. * $p < 0.05$, ** $p < 0.01$, *** $p < 0.001$. X = $p < 0.05$ between groups. The bubble grid shows the reporter test statistics (proportional to size and color intensity) comparing post- relative to pre-overfeeding gene expression. Only pathways significant in at least one diet are shown (<5% false discovery rate).

153x173mm (300 x 300 DPI)

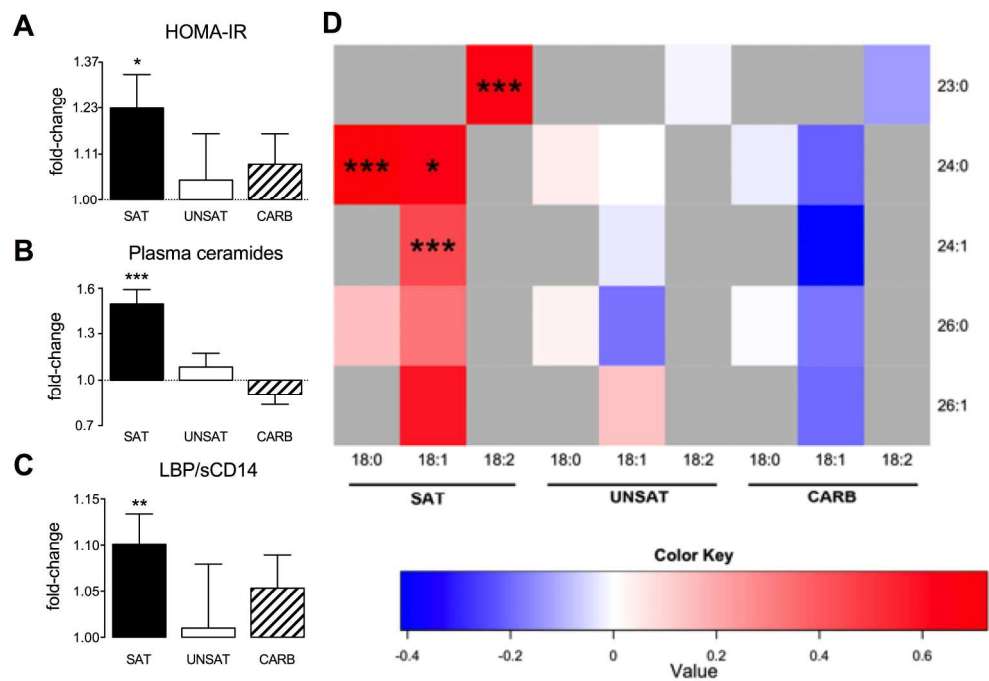


Figure 3. Overfeeding-induced changes in (A) HOMA-IR, (B) total plasma ceramides, (C) LBP/sCD14, and (D) individual plasma ceramides in the groups. Black bars denote the saturated fat (SAT), white bars the unsaturated fat (UNSAT), and hatched bars the simple sugar (CARB) group. The y-axes indicate fold-change of mean values after versus before overfeeding within groups. HOMA-IR = homeostasis model of assessment of insulin resistance, LBP/sCD14 = ratio of lipopolysaccharide-binding protein to soluble cluster of differentiation 14. Data are reported as mean \pm SEM. In the heatmaps, each square indicates the log₂ of the ratio between mean concentrations after versus before for an individual ceramide. The color key denotes the relationship between the color of the heatmap and log₂ of the ratio between the means with 0 indicating no change. The y-axis denotes the fatty acyl chain structure (number of carbon at-oms:number of double bonds) and the x-axis the sphingoid base species. *p<0.05, ** p<0.01, *** p<0.001.

243x167mm (300 x 300 DPI)

Saturated Fat is More Metabolically Harmful for the Human Liver than Unsaturated Fat or Simple Sugars

Panu K. Luukkonen^{1,2}, Sanja Sädevirta^{1,2}, You Zhou^{1,3}, Brandon Kayser⁴, Ashfaq Ali⁵, Linda Ahonen⁵, Susanna Lallukka^{1,2}, Véronique Pelloux⁴, Melania Gaggini⁶, Ching Jian⁷, Antti Hakkarainen⁸, Nina Lundbom⁸, Helena Gylling², Anne Salonen⁷, Matej Orešič^{5,9,10}, Tuulia Hyötyläinen^{5,11}, Marju Orho-Melander¹², Aila Rissanen¹³, Amalia Gastaldelli⁶, Karine Clément^{4,14}, Leanne Hodson¹⁵, Hannele Yki-Järvinen^{1,2,16}

¹Minerva Foundation Institute for Medical Research, Helsinki, Finland; ²Department of Medicine, University of Helsinki and Helsinki University Central Hospital, Helsinki, Finland; ³Systems Immunity University Research Institute and Division of Infection and Immunity, School of Medicine, Cardiff University, Cardiff, United Kingdom; ⁴Sorbonne Universités, INSERM, UMRS 1166, Nutriomics team, ICAN, F-75013, Paris, France; ⁵Steno Diabetes Center, Gentofte, Denmark; ⁶Institute of Clinical Physiology, CNR, Pisa, Italy; ⁷Immunobiology Research Program, Department of Bacteriology and Immunology, University of Helsinki; ⁸Helsinki Medical Imaging Centre, Radiology, Helsinki University Hospital and University of Helsinki; ⁹School of Medical Sciences, Örebro University, Örebro, Sweden; ¹⁰Turku Centre for Biotechnology, University of Turku and Åbo Akademi University, Turku, Finland; ¹¹Department of Chemistry, Örebro University, Örebro, Sweden; ¹²Lund University, Malmö, Sweden; ¹³Obesity Research Unit, Department of Psychiatry, Helsinki University Central Hospital; ¹⁴Assistance Publique-Hôpitaux de Paris (AP-HP), Pitié-Salpêtrière Hospital, Nutrition Department F-75013, Paris, France; ¹⁵Oxford Centre for Diabetes, Endocrinology and Metabolism, University of Oxford, Oxford, UK; ¹⁶Corresponding Author

Table of contents

Adipose tissue transcriptome analyses	3
Gut microbiota analysis	4
References	6
Figure S1	7
Figure S2	8
Figure S3	9
Figure S4	10
Figure S5	11
Table S1	12
Table S2	13
Table S3	14

Adipose tissue transcriptome analyses

Bioinformatics. The Illumina HumanHT12v4 microarray chips (Illumina, San Diego, CA) were annotated using the IlluminaHumanv4.db from Bioconductor. A standard non-specific filtering approach was used to extract genes most likely to be expressed in the tissue and to ultimately limit the number of tests to genes of interest. Specifically, probes without annotation to a gene were removed, and if multiple probes matched to a gene, only the probe with the highest interquartile range across samples was included. Finally, only genes with inter-quartile range greater than the median of all genes were included. KEGG pathways were downloaded from the Molecular Signatures Database (<http://software.broadinstitute.org/gsea/msigdb/collections.jsp#C2>). To limit the number of tests to pathways of interest, unrelated pathways were removed e.g. Huntington's disease.

Statistical analysis. The pre/post comparisons within each diet were computed using LIMMA (1). Specifically, the two factors (time and diet) were converted into a single factor with 6 levels, and after running the full model, contrast tests between levels of interest were performed (e.g. Diet 1-Pre vs Diet 1-Post). The model was analyzed as a multi-level model to account for repeated measures. Array-quality weights were estimated and included in the model. Details of the LIMMA procedure can be found in the comprehensive manual (2).

For the reporter features analysis (3), log₂ fold-change and unadjusted p-values from the LIMMA analysis were used as input. Statistical significance was determined from the null distribution and gene sets were limited to those with more than 3 genes and no more than 200. Otherwise, default parameters were used. Distinctly up- and down-regulated pathways were used to determine pathway enrichment in the specific direction. P-values were adjusted to the Benjamini-Hochberg false discovery rate.

Gut microbiota analysis

Bacterial DNA was extracted from fecal samples using mechanical cell lysis that efficiently extracts bacterial community DNA as previously described (4). Illumina MiSeq paired-end sequencing of the hypervariable V3-V4 regions of the 16S rRNA gene was performed according to the manual from Illumina except that the libraries were prepared with single-step PCR, i.e. by amplifying the 16S rRNA gene fragment together with barcoded primers, the latter adapted from Kozich et al (5). The multiplex PCR reaction is comprised of 1 ng/ul template, 1X Phusion® Master Mix (ThermoFisher, F-531L), 0.25 uM V3-V4 locus specific primers and 0.375 uM dual-index barcodes. The PCR was run under the following settings: 98 °C for 30 s, 27 cycles of 98 °C for 10 s, 62 °C for 30 s, 72 °C for 15 s and finally 10 min at 72 °C, where after the samples were stored at 4 °C. The size of the PCR product was expected to be ~640 base pairs (bp) and verified on a Bioanalyzer DNA 1000 chip (Agilent Technology, Santa Clara, CA, USA). The PCR clean-up was performed with AMPure XP beads (Beckman Coulter, Copenhagen, Denmark) and confirmation of the right size of the target was performed on a Bioanalyzer DNA 1000 chip (Agilent Technology, CA, USA). The pooled libraries were sequenced at the sequencing unit of the Institute for Molecular Medicine Finland (FIMM), Helsinki, Finland with an Illumina MiSeq instrument using paired end 2 × 300 bp reads and a MiSeq v3 reagent kit with 5% PhiX as spike-in.

Sequencing data preprocessing, analysis and statistics

The forward reads were truncated to length of 150 bases with `ProcessReads` command. We used default settings for minimum quality score and maximum expected errors. Reads with prevalence below 0.01% were removed. Chimera removal and dereplication of the reads was done using USEARCH8 (6). Truncated, filtered and dereplicated reads were annotated using the Silva database (7). The median read count per sample after preprocessing

was 68797 (range 296 –148 604). The data analysis was done without rarefaction or transformations utilizing statistical and visualization tools included in the mare-package (8). The number of reads was used as an offset in all statistical models. Community dissimilarity was estimated with principal coordinates analysis (PCoA) using Bray-Curtis dissimilarity as the distance measure. PCoA was calculated with capscale function of R package vegan and Bray-Curtis dissimilarities with function vegdist of the same package (9). Permutational multivariate analysis of variance using distance matrices was performed with adonis function in package vegan to calculate the relative contribution of different factors in the microbiota variation. Taxonomic richness was estimated as the number of observed OTUs after clustering the reads to operational taxonomic units (OTUs) using USEARCH8. Comparison of the abundance of bacterial genera between two time points in each intervention group was performed using generalized linear mixed models within “GroupTest” function of the mare package using subject as the random factor. This function uses the glmmADMB package (generalized linear mixed models built on AD Model Builder) of R software on background and assumes negative binomial distribution of abundance.

REFERENCES

1. Smyth GK: Linear models and empirical bayes methods for assessing differential expression in microarray experiments. *Stat Appl Genet Mol Biol* 2004
2. Smyth GK, Ritchie M, Thorne N, Wettenhall J, Shi... W: *Limma: Linear Models for Microarray and RNA-Seq Data User's Guide*. Citeseer 2002
3. Våremo L, Nielsen J, Nookaew I: Enriching the gene set analysis of genome-wide data by incorporating directionality of gene expression and combining statistical hypotheses and methods. *Nucleic Acids Res* 41:4378-4391, 2013
4. Salonen A, Nikkila J, Jalanka-Tuovinen J, Immonen O, Rajilic-Stojanovic M, Kekkonen RA, et al. (2010). Comparative analysis of fecal DNA extraction methods with phylogenetic microarray: effective recovery of bacterial and archaeal DNA using mechanical cell lysis. *J Microbiol Methods*. 81(2):127-34.
5. Kozich JJ, Westcott SL, Baxter NT, Highlander SK, Schloss PD. (2013). Development of a dual-index sequencing strategy and curation pipeline for analyzing amplicon sequence data on the MiSeq Illumina sequencing platform. *Appl Environ Microbiol*. 79(17):5112-20.
6. Edgar RC. (2010). Search and clustering orders of magnitude faster than BLAST. *Bioinformatics*. 26(19):2460-1.
7. Quast C, Pruesse E, Yilmaz P, Gerken J, Schweer T, Yarza P, et al. (2012). The SILVA ribosomal RNA gene database project: improved data processing and web-based tools. *Nucleic Acids Res*. gks1219.
8. Korpela K. (2016). *mare: Microbiota Analysis in R Easily*. R package version 10" 23-Apr-2016.
9. Oksanen JFGB, R. Kindt, P. Legendre, P.R. Minchin, R.B. O'Hara, G.L. Simpson, P. Solymos, M.H.H. Stevens, H.Wagner. (2011). Package 'vegan' version 2.0-2.

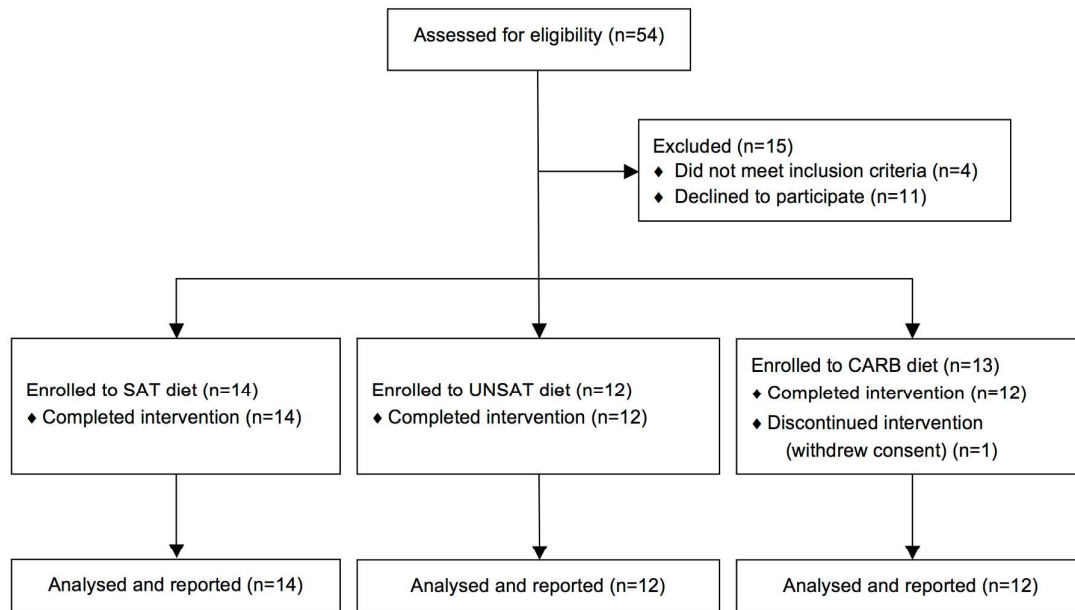
Supplementary Figures

Figure S1. Study flow chart. A total of 54 subjects were assessed for eligibility, 39 of whom were considered eligible. One subject withdrew from the study. Data were collected and analyzed on 14 subjects enrolled to the SAT diet, 12 subjects enrolled to the UNSAT diet, and 12 subjects enrolled to the CARB diet.

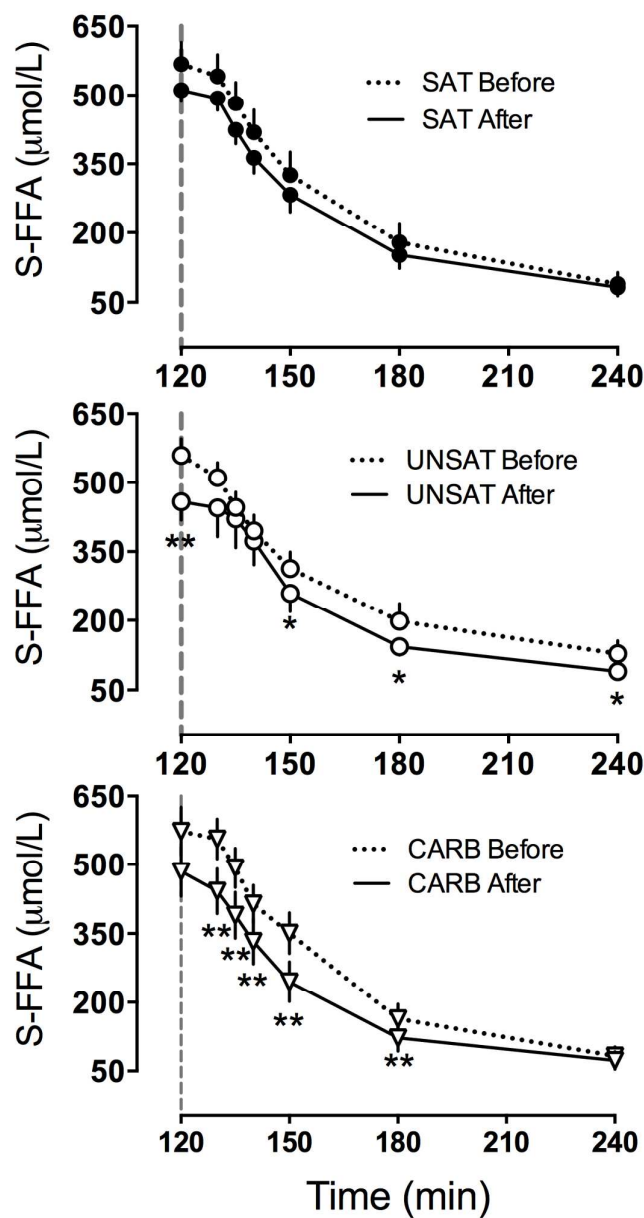


Figure S2. Serum free fatty acid (FFA) concentrations during euglycemic hyperinsulinemic clamp before and after the overfeeding. SAT = saturated fat (panel on the top), UNSAT = unsaturated fat (panel in the middle), CARB = simple sugar group (panel on the bottom). The x-axes denote serum FFA concentration and the y-axes time from the beginning of the study (euglycemic hyperinsulinemic clamp was started at 120 minutes). * $p < 0.05$, ** $p < 0.01$.

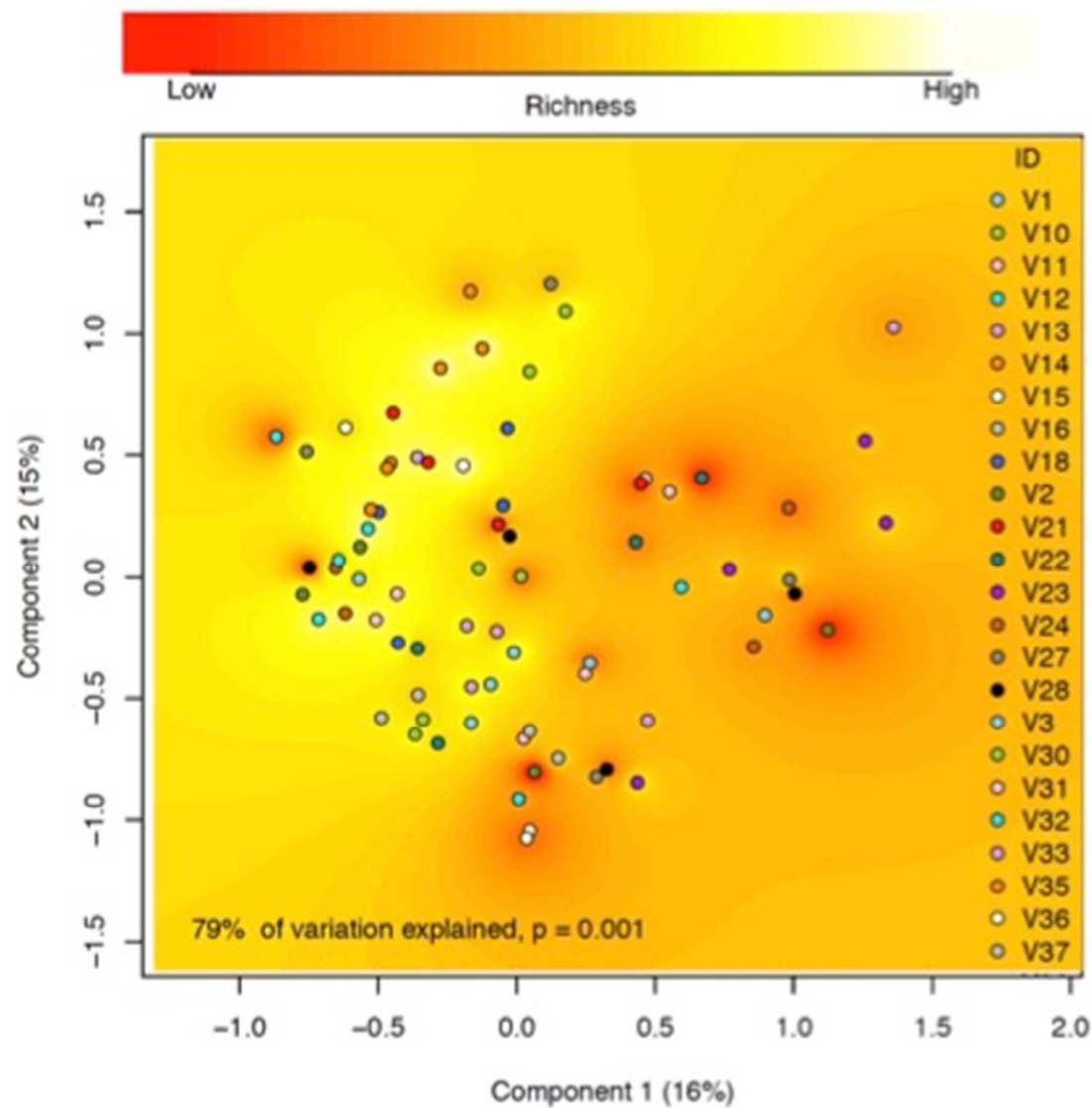


Figure S3. Principal coordinates analysis (PCoA) plot based on Bray-Curtis dissimilarity of all the microbiota samples, coloured according to the subject. The background colour indicates microbiota richness. Permutational multivariate analysis of variance was used to calculate the explanatory power of the subject.

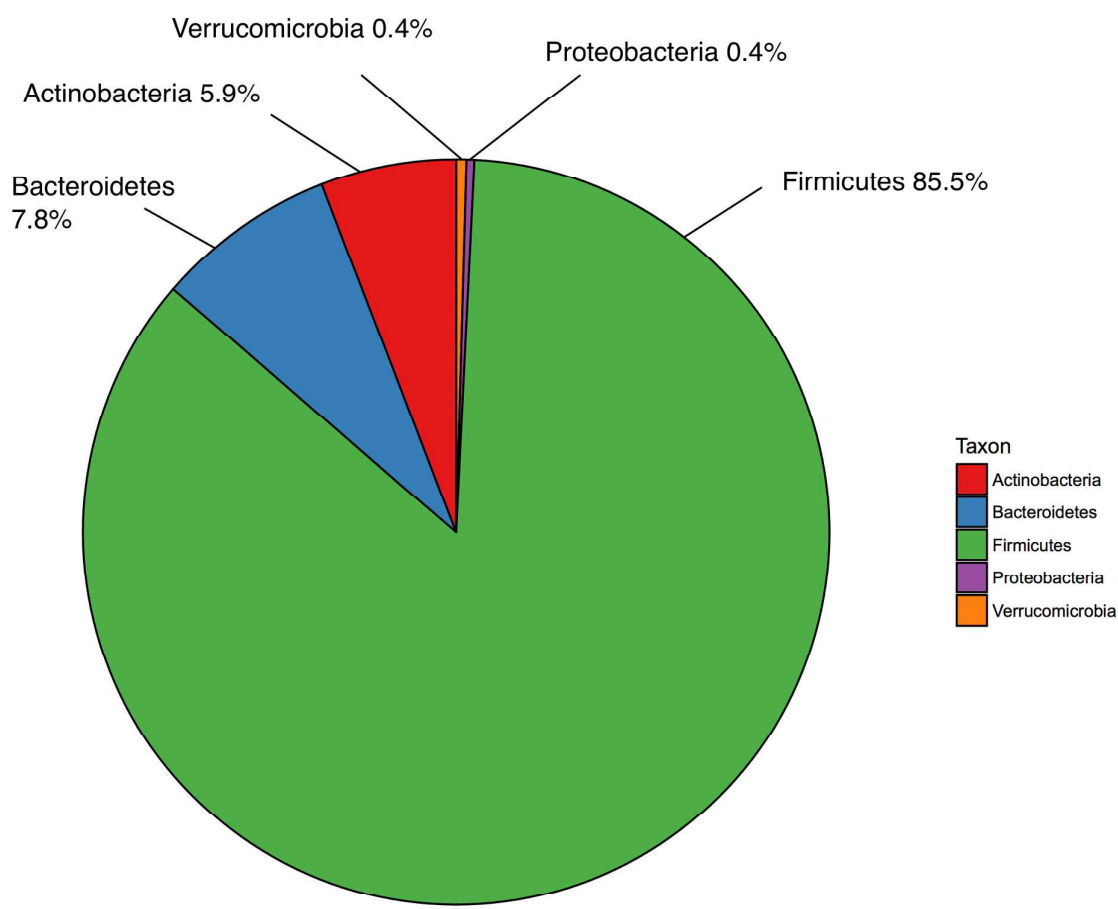


Figure S4. Microbiota composition in the study subjects at baseline.

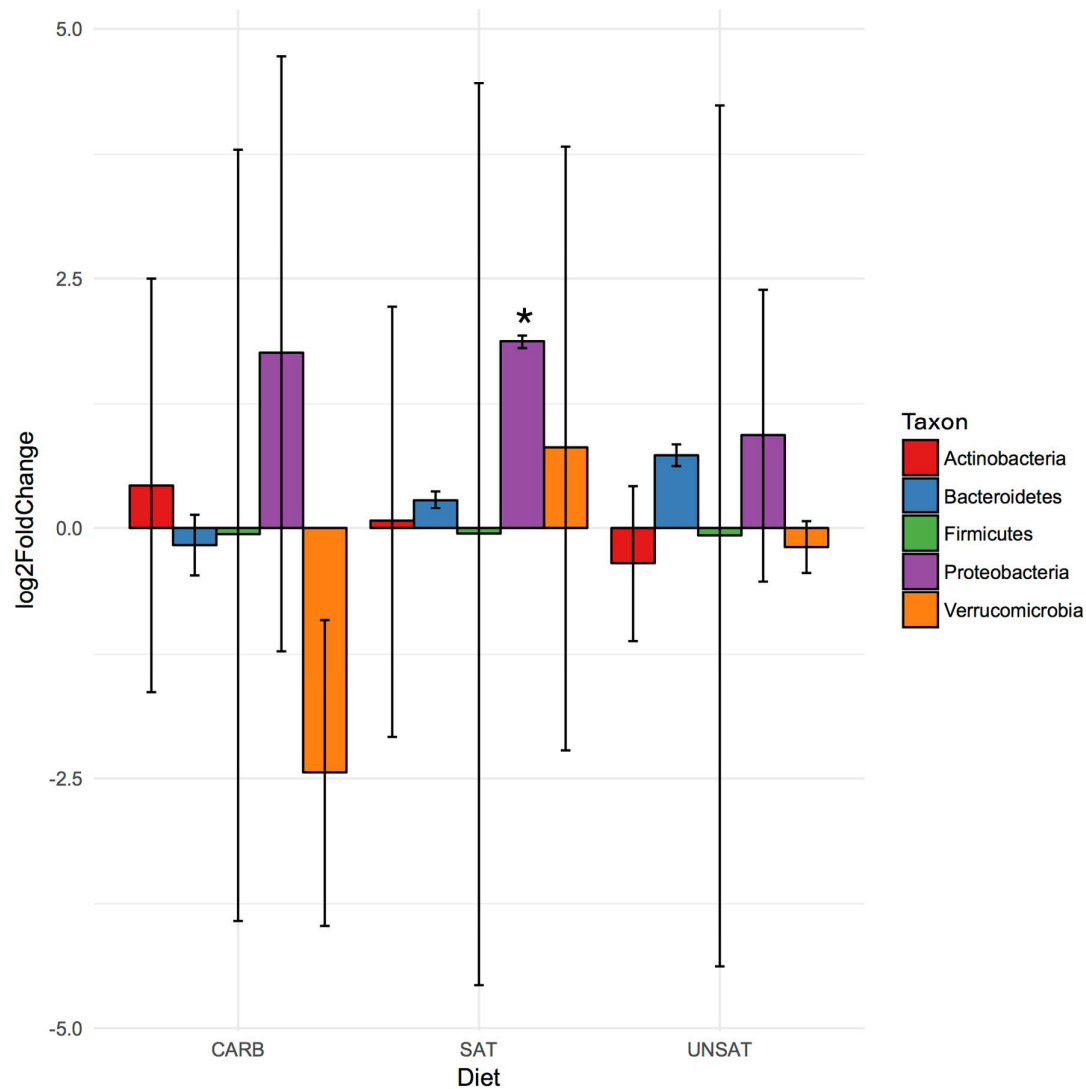


Figure S5. Mean log₂ fold-changes (± standard error) of the bacterial phyla in the groups. The fold-changes and their statistical significance before and after overfeeding are based on negative binomial models. Significant difference is indicated by the asterisk (p<0.05).

Table S1. Dietary profiles of the groups before and after the overfeeding based on food records.

	SAT (n=14)		UNSAT (n=12)		CARB (n=12)	
	Before	After	Before	After	Before	After
Energy intake (MJ/day)	7.61 (6.02 – 9.18)	11.67 (9.87 – 13.41)*	8.88 (7.99 – 10.89)	12.07 (11.05 – 13.54)*	8.20 (7.36 – 10.49)	12.15 (11.14 – 15.79)*
Protein intake (E%)	19.8 (15.2 – 21.7)	15.0 (11.5 – 15.5)*	18.8 (16.2 – 20.9)	13.2 (11.9 – 15.3)*	19.5 (16.1 – 22.0)	11.4 (9.4 – 14.5)*
Carbohydrate intake (E%)	38.4 (32.2 – 41.3)	25.9 (23.0 – 32.2)*	34.5 (31.6 – 39.7)	22.7 (19.3 – 28.9)*	40.0 (36.9 – 47.8)	63.7 (58.1 – 67.5)*
Fat intake (E%)	39.4 (36.5 – 42.1)	58.9 (53.1 – 61.1)*	38.8 (32.0 – 43.5)	59.7 (53.6 – 63.6)*	35.6 (31.5 – 42.4)	23.8 (19.6 – 25.8)*
Saturated fat intake (E%)	12.9 (11.7 – 14.6)	32.7 (27.6 – 35.5)*	12.9 (11.0 – 16.0)	14.3 (13.5 – 18.3)	13.1 (11.7 – 15.2)	8.3 (6.5 – 9.7)*
Monounsaturated fat intake (E%)	13.9 (11.9 – 16.8)	12.8 (11.9 – 14.9)	13.2 (11.2 – 15.9)	27.7 (23.1 – 30.4)*	12.1 (10.8 – 14.4)	8.5 (6.4 – 9.4)*
Polyunsaturated fat intake (E%)	6.7 (6.4 – 8.5)	4.5 (4.0 – 5.2)*	5.1 (4.9 – 9.2)	11.4 (9.5 – 13.5)*	5.6 (5.1 – 7.0)	3.4 (3.2 – 4.0)*

Data are in median (25th-75th percentile). No differences between groups at baseline (Kruskal-Wallis test). * $p < 0.05$ in Wilcoxon Signed Rank test between Before and After within a group.

Table S2. Baseline fatty acid compositions of VLDL-TG according to groups.

Total	SAT (n=14)	UNSAT (n=12)	CARB (n=12)
C14:0 (%)	1.8 ± 0.2	2.0 ± 0.2	2.3 ± 0.2
C16:0 (%)	26.2 ± 1.0	27.0 ± 0.9	27.8 ± 0.8
C16:1 n-7 (%)	4.6 ± 0.5	4.4 ± 0.3	5.2 ± 0.5
C18:0 (%)	3.1 ± 0.3	3.3 ± 0.3	3.1 ± 0.3
C18:1 n-9 (%)	37.6 ± 0.9	37.8 ± 0.9	36.9 ± 0.9
C18:2 n-6 (%)	14.8 ± 1.0	13.7 ± 0.7	13.0 ± 0.9

Data are in means ± SEM. There were no significant differences in any variable between the groups.

Table S3. Plasma ceramide concentrations before and after overfeeding in the groups.

Lipid name	SAT			UNSAT			CARB		
	Mean Before	Mean After	Q value	Mean Before	Mean After	Q value	Mean Before	Mean After	Q value
Cer(d16:2(4E,6E)/22:1(13Z)(2OH))	6.78643	9.11274	0.36	7.71353	9.27031	0.96	9.89585	9.68906	0.74
	+/-	+/-		+/-	+/-		+/-	+/-	
	0.96342	1.33409		0.87035	1.25029		1.71856	1.3074	
Cer(d18:0/24:0)	4.10406	6.50034	0.0052	3.99065	4.35705	0.97	4.52223	4.28191	0.88
	+/-	+/-		+/-	+/-		+/-	+/-	
	0.38621	0.57013		0.48144	0.47258		0.48002	0.52112	
Cer(d18:0/h24:0)	1.06967	1.56036	0.011	1.19847	1.18781	0.99	1.36244	1.32872	0.72
	+/-	+/-		+/-	+/-		+/-	+/-	
	0.06491	0.09943		0.08729	0.103		0.10395	0.17257	
Cer(d18:0/h26:0)	0.76885	0.88989	0.59	0.78448	0.81856	0.99	0.84401	0.85801	0.98
	+/-	+/-		+/-	+/-		+/-	+/-	
	0.0358	0.09756		0.04429	0.07748		0.05797	0.09246	
Cer(d18:1/24:0)	2.84316	4.15985	0.046	3.25284	2.86855	1	3.72058	3.50024	0.59
	+/-	+/-		+/-	+/-		+/-	+/-	
	0.31666	0.34251		0.35171	0.39869		0.40393	0.48568	
Cer(d18:1/24:1(15Z))	1.07751	1.54825	0.0026	1.27397	1.25989	0.96	1.37157	1.16452	0.59
	+/-	+/-		+/-	+/-		+/-	+/-	
	0.10154	0.14089		0.11128	0.13142		0.13407	0.11646	
Cer(d18:1/26:0)	2.07704	3.1566	0.53	2.45716	2.53512	0.97	2.40496	2.15873	0.72
	+/-	+/-		+/-	+/-		+/-	+/-	
	0.17362	0.33601		0.2555	0.33441		0.14202	0.18681	
Cer(d18:1/26:1(17Z))	0.45668	0.59172	0.29	0.46159	0.50701	0.97	0.54902	0.52781	0.7
	+/-	+/-		+/-	+/-		+/-	+/-	
	0.02678	0.07791		0.03213	0.05571		0.04149	0.04814	
Cer(d18:2/23:0)	0.86491	1.31764	0.0076	1.08901	1.09294	0.99	1.28808	1.1395	0.83
	+/-	+/-		+/-	+/-		+/-	+/-	
	0.10664	0.09732		0.10233	0.12264		0.18622	0.1233	
Cer(m18:0/24:0)	1.28955	2.09629	0.0018	1.43542	1.46197	0.99	1.61955	1.56872	0.93
	+/-	+/-		+/-	+/-		+/-	+/-	
	0.18757	0.21783		0.24432	0.20338		0.14476	0.17573	
Cer(m18:1(4E)/24:0)	1.02325	1.60998	0.034	1.25439	1.27772	0.99	1.38289	1.4231	0.92
	+/-	+/-		+/-	+/-		+/-	+/-	
	0.12517	0.1801		0.22107	0.20404		0.1927	0.19509	
Cer(m18:1(4E)/24:1(15Z))	1.96867	2.60291	0.011	1.99667	1.89242	0.97	2.96021	2.20154	0.7
	+/-	+/-		+/-	+/-		+/-	+/-	
	0.13806	0.17806		0.21621	0.16879		0.46321	0.2227	
Cer(m18:1(4E)/26:1(17Z))	2.69515	4.29115	0.02	3.31751	3.34588	0.97	3.42067	3.05406	0.72
	+/-	+/-		+/-	+/-		+/-	+/-	
	0.29105	0.37047		0.42431	0.42823		0.24066	0.29993	